RAYLEIGH-TAYLOR INSTABILITY WITH SELF-GENERATED MAGNETIC FIELD AND THERMAL CONDUCTION IN 2D

F. Modica[1], T. Plewa[1], A.V. Zhiglo[2]
[1]Florida State University, Tallahassee, FL, USA;
[2]National Science Center "Kharkov Institute of Physics and Technology", Kharkov, Ukraine
E-mail: azhiglo@gmail.com

High energy density laboratory experiments on Rayleigh-Taylor instability (RTI) [1] in nonlinear regime show the plasma behavior significantly different from classical simulation results. We include the effects of self-generated magnetic field and heat conduction in simulations aiming to improve agreement with experiments. We find maximum magnetic fields generated ~11MG (β=0.091) without heat conduction (κ=0), field growth saturated by t=20ns; and ~1.7 MG with heat conduction taken into account. Strong magnetic fields in κ=0 simulations affect flow dynamics, new modes are generated. Effect of weaker magnetic fields in simulations with physical values of κ is insignificant; the main difference with classical RTI simulations is suppressed small scale features. In none of the simulations are mass extensions observed.

PACS: 52.25.Xz, 52.30.Cv, 52.35.Py, 52.57.-z, 52.65.-y, 44.10.+i, 72.15.Jf

INTRODUCTION

A hydrodynamic system in which a light fluid supports a denser fluid in a gravitational field is subject to Rayleigh-Taylor instability (RTI). A small perturbation of the horizontal interface between the fluids grows exponentially with time in a linear regime. When its amplitude A becomes comparable to the perturbation wavelength λ characteristic RTI morphology starts developing, with spikes of the denser fluid (called fluid 2 below) sinking in the lighter one (labeled with index 1), separated by rising bubbles of the lighter fluid. Noticeably different picture is however observed in high energy density laboratory astrophysics (HEDLA) experiments, designed to mimic RTI in core-collapse supernovae ejecta. In experiments [1] a cylindrical target made of two plastics separated by a thin tracer layer at the sinusoidally perturbed planar interface (λ=71 μm, $A(t=0) = 5$ μm) was illuminated by an intense laser; irradiance of $\sim 9\times10^{14}$ W cm^{-2} was created for 1 ns. Blast wave created after the material evaporation overruns the interface, the lighter material gets decelerated by the denser one (both turned into plasmas); this making the interface RT unstable, equivalent acceleration (playing the role of roughly uniform gravitational field) being $g \sim 2\times10^{14}$ cm s^{-2}. "Sinking" spikes of the denser plasma were observed lacking characteristic structure on small scales, including typically developing Kelvin-Helmholtz instability (KHI) waves at side shear interface of fluid 2 spikes moving through fluid 1. "Rising" "bubbles" of the lighter material were likewise observed nearly cylindrical, with mushroom-like head formation (as well as smaller scale structures) significantly suppressed.

Magnetic fields are known to suppress RTI in certain situations. Say, the growth rate in a uniform magnetic field tangential to the interface in linear regime is smaller than in the absence of magnetic field [2]:

$$n^2 = gk\frac{\rho_2 - \rho_1}{\rho_2 + \rho_1} - \frac{(\mathbf{B}\cdot\mathbf{k})^2}{2\pi(\rho_2 + \rho_1)},$$

where **k** is the perturbation wave-vector, **B** the magnetic induction, ρ_1 and ρ_2 are the densities of the light and the dense fluids. Thermal conduction can also suppress the RTI development by diffusing density gradients near the interface, especially when the two materials are of similar mean atomic weight, so most of the density variation is due to the difference in temperature of the two fluids.

We include the magnetic and thermal conduction effects, to see if that can account for the discrepancy with experiments. Magnetic fields are generated via Biermann-battery effect [3] (2nd term in the RHS of Eq. 3), as the gradients of electron number density and temperature are not parallel near the interface as RTI develops.

1. MODEL AND NUMERICAL METHOD

For numerical simulations we use the Proteus code (a branch of the FLASH code [4]), with new modules added for describing non-ideal MHD effects and anisotropic heat conduction. One-fluid one-temperature MHD model is used; viscosity and resistivity are neglected. The equations solved are continuity equation, Euler equation for the plasma velocity **V**, with gravity and magnetic force,

$$\frac{\partial(\rho V_i)}{\partial t} + \frac{\partial}{\partial x_k}\left(\rho V_i V_k - \frac{B_i B_k}{4\pi}\right) + \frac{\partial P}{\partial x_k} = \rho g_i, \quad (1)$$

energy balance equation for the total energy density E

$$\frac{\partial(\rho E)}{\partial t} + \frac{\partial}{\partial x_k}\left((\rho E + P)V_k - \frac{B_i B_k}{4\pi}V_i\right) = \rho\mathbf{V}\mathbf{g} + \nabla\mathbf{q}_T, \quad (2)$$

generalized Ohm's law for magnetic field **B** evolution

$$\frac{\partial\mathbf{B}}{\partial t} = \frac{c}{e}\nabla\times\left(\mathbf{V}\times\mathbf{B} + \frac{\nabla P_e}{n_e} - \frac{(\nabla\times\mathbf{B})\times\mathbf{B}}{4\pi n_e} - \frac{\mathbf{R}_T}{n_e}\right); \quad (3)$$

div **B** = 0 is ensured at every integration step. Total pressure P as well as E include magnetic pressure and energy density. P_e and n_e denote electron pressure and number density. $\mathbf{R}_T$ and $\mathbf{q}_T$ are the thermal force and heat flux, both given as linear (but anisotropic when $\mathbf{B} \neq 0$, preferentially oriented along **B** in magnetized plasmas) combinations of components of ∇T; explicit expressions and more on the model can be found in [5].

2. RESULTS

Simulations reported are performed on a [0;71]×[0;284] μm domain; periodic boundary conditions are imposed

in x. Amplitude of initial sinusoidal perturbation between the two fluids with $\rho_1=1$, $\rho_2=2$g cm^{-3} is $A=5$ μm. $\mathbf{g}=(0;-2\times10^{14}$ cm s$^{-2})$, minimum ambient pressure is 5×10^{11} dyn cm^{-2}. Temperature varied between 3.8×10^4 and 1.3×10^6 K at $t=0$, determined by hydrostatic condition and the (Thomas-Fermi) equation of state used. Resolution varied between 20 and 160 computation cells per domain width, corresponding setups denoted L20 to L160. Unsplit staggered mesh (USM) MHD solver of FLASH was used.

Fig. 1 shows density distribution for classical RTI ($\mathbf{B}=\kappa=0$), RTI with self-generated magnetic field and $\kappa=0$, and RTI in the full problem. Boundaries of mixed region and $|B_z|$ distribution are shown in Fig. 2. Fig. 3 shows the evolution of x-averaged B_z with time.

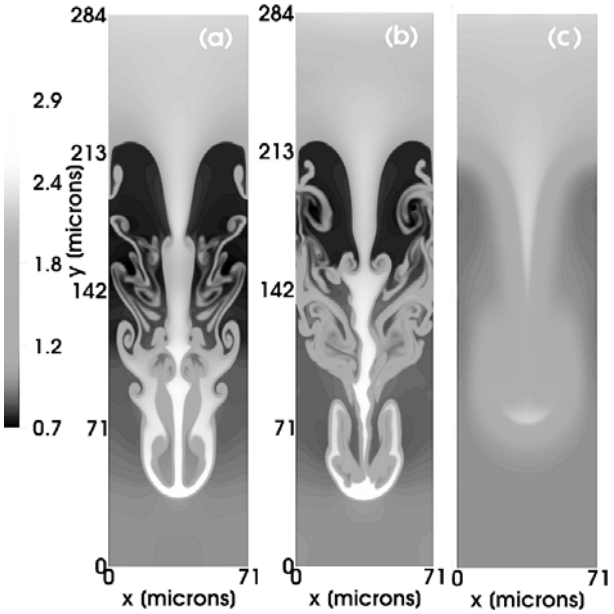

Fig. 1. Density distribution at t=35 ns, tone-coded; L160 model. (a) Pure hydrodynamics: $\mathbf{B}=\kappa=0$; (b) Hydro with self-generated **B**, *κ=0; (c) full problem*

Distributions of hydrodynamic quantities at $\mathbf{B}=0$ and physical value of heat conductivity κ are visually indistinguishable from those of the full problem, thus are not shown. These distributions do not converge pointwise with resolution when small-scale cutoff due to dissipation is absent; this is observed in our $\kappa=0$ runs. Certain averaged characteristics that describe mixing in the interface region should converge according to classical RTI studies. Fig. 4 shows the dependence of the lateral averages of density (in x; as a function of the vertical coordinate) on simulation resolution. It is seen that the problem with the heat conduction is already well-resolved at 20 cells per the domain width, whereas in the setups with $\kappa=0$ the difference can be seen even between L80 and L160 models at some y, although near the bubble and spike tips physics is seen already well-resolved in L40 setup.

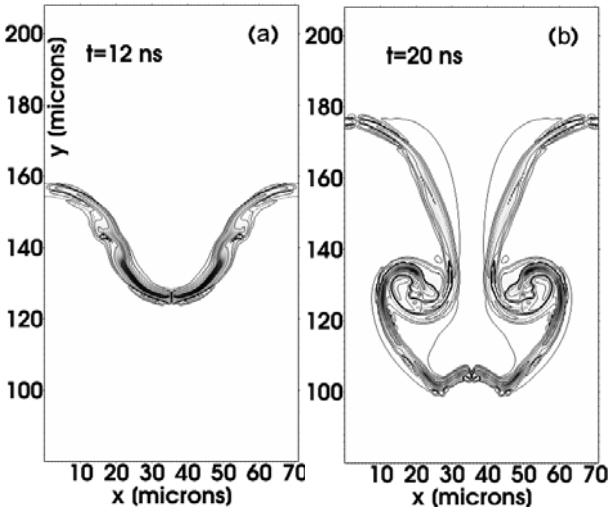

Fig. 2. RTI at κ=0, L160. Top and bottom dashed lines: mass fraction of heavy fluid 0.99 and 0.01. $|B_z|$: tone coded (larger $|B_z|$ is darker), and solid contour lines, equidistant (step 0.5 dex) in $\lg|B_z|$, 1st one at $\lg|B_z|=4.5$

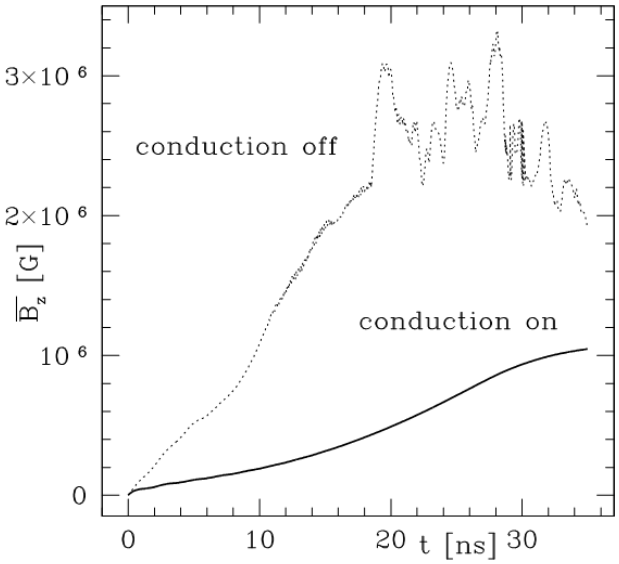

Fig. 3. Maximum x-averaged B_z vs time; L160. Dotted: κ=0, solid: full problem

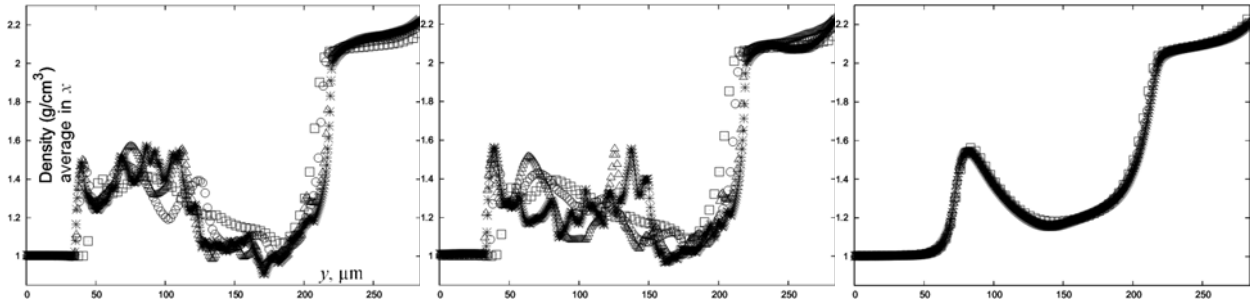

Fig. 4. $\langle\rho\rangle_x(y)$ for L20 (squares), L40 (circles), L80 (triangles), and L160 (asterisks) models at t = 35 ns. Left: Pure hydrodynamics: $\mathbf{B}=\kappa=0$; *middle: hydro with self-generated* **B**, *κ=0; right: full problem*

In Fig.5 perturbation growth with time is shown. It is seen only marginally affected by self-generated magnetic field; heat conduction decreases the mixed layer width by ~20%. No significant mass extension [1] is observed.

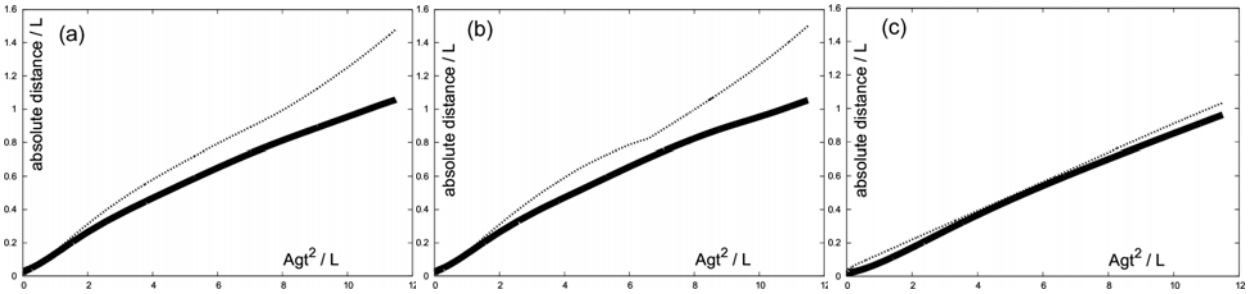

Fig.5. Normalized to the domain width L distance of the RT spikes (solid) and bubbles (dashed) from their initial location vs Agt^2/L, A denoting Atwood number. (a) **B**=κ=0. *(b) hydro with self-generated* **B**, κ=0; *(c) full problem*

CONCLUSIONS

2D 1-fluid simulations of RTI with magnetic field **B** generation and heat conduction according to Braginskii's eqs. with resistivity and viscosity neglected show subtle dynamical effects due to **B**, interface broadening due to heat conduction, with development of structures finer than the interface width suppressed. The former effects include additional mode in RTI (seen developing in Fig. 2,b at $x \approx \lambda/4$, at the peak of magnetic pressure, leading to a dent in the RT spike at t = 20 ns); the fields remain weak in a sense that transport coefficients stay unaffected by **B** to within 2%. Laterally averaged |**B**| reaches ~11 MG (β=0.091) at κ=0 and ~1.7 MG with heat conduction taken into account; in the latter case **B** does not play a significant role in RTI dynamics. These values agree well with recent experiments. More details and tests of the code can be found in [6].

FM and TP were supported in part by the DOE grant DE-FG52-09NA29548 and the NSF grant AST-1109113.

REFERENCES

1. C.C. Kuranz, R.P. Drake, et.al. Spike morphology in blast-wave-driven instability experiments// *Phys. Plasmas*. 2010, v.17, p. 052709-1-15.
2. S. Chandrasekhar. *Hydrodynamic and hydromagnetic stability*. Oxford: Clarendon Press, 1961.
3. L. Biermann. Über den Ursprung der Magnetfelder auf Sternen und im interstellaren Raum // *Z. Naturforschung A*. 1950, v.5, p.65.
4. B. Fryxell, K. Olson, et al. FLASH: An Adaptive Mesh Hydrodynamics Code for Modeling Astrophysical Thermonuclear Flashes// *ApJS*. 2000, v.131, p. 273-334.
5. S.I. Braginskii. Transport Processes in a Plasma// *Reviews of Plasma Physics, v.1* / Consultants Bureau, New York, 1965, v.1, p. 205.
6. M.J.-E. Manuel, C.K. Li, et. al. First Measurements of Rayleigh-Taylor-Induced Magnetic Fields in Laser-Produced Plasmas // *Phys. Rev. Lett*. 2012, v.108, p. 255006-1-5.

Article received 19.09.12

НЕУСТОЙЧИВОСТЬ РЭЛЕЯ-ТЭЙЛОРА С САМОГЕНЕРИРУЕМЫМ МАГНИТНЫМ ПОЛЕМ И ТЕПЛОПРОВОДНОСТЬЮ В 2D

F. Modica, T. Plewa, A.B. Жигло

В экспериментах неустойчивости Рэлея-Тэйлора (НРТ) в лабораториях высоких плотностей энергии [1] поведение жидкости существенно отличается от классических результатов численного моделирования. С целью улучшить согласие с экспериментами мы включили в моделирование эффекты самогенерирующегося магнитного поля и теплопроводности. Максимальное магнитное поле получено ~11 MG (β=0.091) в отсутствие теплопроводности (κ=0), рост поля насыщается к t=20 ns; и ~1.7 MG при учтённой теплопроводности. Сильное магнитное поле в модели с κ=0 меняет динамику неустойчивости, генерируются новые моды. Эффект более слабого поля в моделировании с физическими значениями κ несуществен; основное отличие от классической НРТ заключается в подавлении мелкомасштабных структур. Удлинения РТ структур в моделях не наблюдалось.

НЕСТІЙКІСТЬ РЕЛЕЯ-ТЕЙЛОРА З МАГНІТНИМ ПОЛЕМ, ЩО САМОГЕНЕРУЄТЬСЯ, ТА ТЕПЛОПРОВІДНІСТЮ В 2D

F. Modica, T. Plewa, A.B. Жигло

У експериментах нестійкості Релея-Тейлора (НРТ) в лабораторіях великих щільностей енергії [1] поведінка рідини суттєво відрізняється від класичних результатів чисельного моделювання. Для узгодження з експериментами ми включили в моделювання ефекти магнітного поля, що самогенерується, та теплопровідності. Максимальне магнітне поле одержано ~11 MG (β=0.091) за відсутностю теплопровідності (κ=0), зростання поля насичується до t=20 ns; та ~1.7 MG, коли теплопровідність врахована. Сильне магнітне поле в моделі з κ=0 змінює динаміку нестійкості, генеруються нові моди. Ефект більш слабкого поля при моделюванні з фізичними значеннями κ несуттєвий; головною відмінністю від класичної НРТ є нерозвиненість дрібномасштабних структур. Подовження РТ структур в моделях не помічалося.